Edelweiss Applied Science and Technology
ISSN: 2576-8484
Vol. 8, No. 6, 5236-5253
2024
Publisher: Learning Gate
DOI: 10.55214/25768484.v8i6.3147

Bio convection heat transfer in Sisko nanofluid past a stretching cylinder with Soret and Dufour effects

Khuram Rafique[1], Gamal Elkahlout[2*] Ayesha Rehman[1], Shamaila Kanwal[1]
[1]Department of Mathematics, University of Sialkot, Sialkot 51040, Pakistan. Email: khurram.rafique1005@gmail.com (K.R.) Ayesharehmankhalid@gmail.com (A.R.) shamaila3355@gmail.com (S.K.)
[2]School of Business Studies, Arab Open University, Riyadh, Saudi Arabia; g.elkahlout@arabou.edu.sa (G.E.)

Abstract: The present flow model provides useful information for the production of nano-biomaterials, medical treatment, materials science current research model has been utilized. The unique thermal mechanisms of nanoparticles have garnered significant attention from researchers in recent years. These versatile materials have numerous applications in various fields, including cooling and heating control processes, solar systems, energy production, nanoelectronics, hybrid-powered motors, cancer treatments, and renewable energy systems. Furthermore, the bioconvection of nanofluids has exciting implications for bioengineering and biotechnology, with potential uses in biofuels, biosensors, and enzymes. The aim of this study is to investigate the flow behaviour of bioconvection Sisko nanofluid flow through a stretching cylindrical surface. Further, the analysis has been modified by including the effects of Soret and Dufour. The highly nonlinear and coupled differential equations were numerically solved using a BVP4c solver to simulate the problem. The effects of different flow parameters on velocity, temperature, and concentration distributions are examined and illustrated through graphical results. It is clearly observed from the results that Soret impacts increases the concentration distribution. Moreover, Dufour impacts increment increases the temperature of the flow.
Keywords: *Bioconvection, Motile microorganisms, Sisko nanofluid, Soret and dufour effects, Stretching cylinder.*

1. Introduction

In today's era of rapid scientific advancements, the Sisko model has emerged as a vital tool for understanding the behaviour of non-Newtonian fluids at the nanoscale. As a non-Newtonian fluid, Sisko fluid exhibits unique properties that are crucial for various applications, including drug delivery, tissue engineering, and biomedical devices. Its ability to simulate the flow dynamics of biofluids like blood and mucus has far-reaching implications for the development of targeted therapies and personalized medicine.

Moreover, the Sisko model is also being explored for its potential in enhancing the performance of energy storage devices, such as batteries and supercapacitors, and improving the efficiency of industrial processes, like oil recovery and transportation. With its versatility and accuracy, the Sisko model is poised to revolutionize various fields and transform the way we approach complex fluid dynamics challenges. Researchers have explored the behaviour of Sisko fluid in various scenarios, including laminar and turbulent flows, boundary layers, and heat transfer.

Adesanya et al. [1] conducted a computational study on reaction-driven magneto-convective flow in Sisko fluid. Hafez et al. [2] investigated the Electrohydrodynamic (EHD) peristaltic flow of Sisko fluid, examining the combined effects of convection and endoscopy. Islam et al. [3] numerically analyzed convective energy transfer in Sisko fluid flow over an extending device, accounting for radiation and heat dissipation effects. Khan et al., [4] inspected the unsteady flow of a Sisko fluid in a moving cylindrical tube. Nisha et al., [5] discovered the effects of electro-osmotic forces, activation energy, and chemical reactions on the flow of Sisko fluid above a Darcy-Forchheimer absorbent enlarging cylinder.

* Correspondence: g.elkahlout@arabou.edu.sa

Prasannakumara et al., [6] have conducted a study on the numerical analysis of MHD flow and nonlinear radiative heat transfer in Sisko nanofluid over a nonlinear stretching sheet. Upreti et al., [7] investigated the effects of viscous dissipation and suction on convective heat transfer in Sisko fluid flow over a stretching surface, providing valuable insights into the numerical assessment of this phenomenon. Imran et al., [8] investigated the thermal transport properties in Sisko fluid flow under peristaltic motion. Bisht et al., [9] examined the effects of solar radiation on radiative heat transfer in MHD Sisko nanofluid flow.

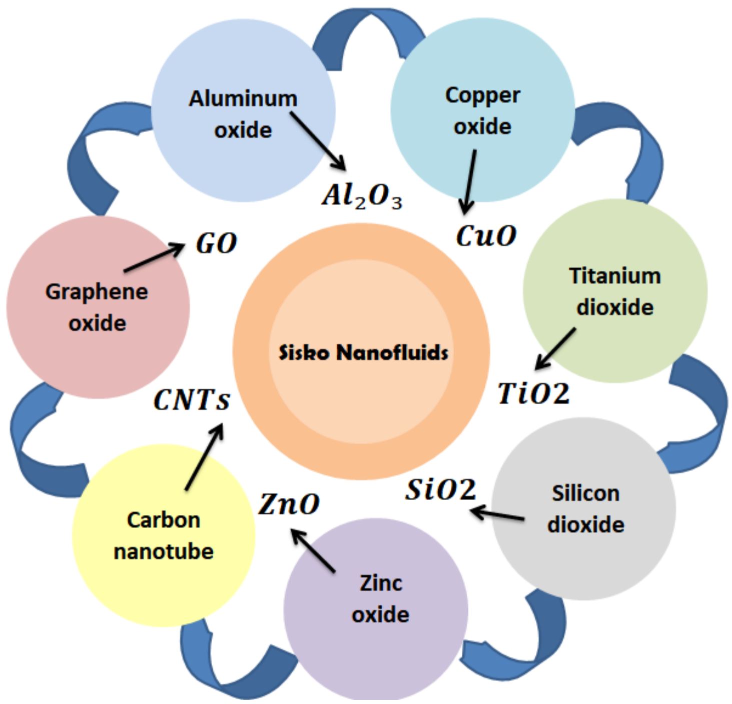

Figure 1.
Some common nanoparticles used in Sisko nanofluid.

Nanofluid is a modern type of fluid that combines a base fluid with nano-sized particles of various metals, such as copper, aluminium, and silicon. The primary purpose of adding nanoparticles to the base fluid is to enhance its thermal conductivity, as conventional heat transfer fluids like oil, ethylene glycol, water, and engine oil have naturally poor thermal conductivity. To improve thermal conductivity, numerous experiments have been conducted, including changing the geometry of the problem and adding different-sized metallic particles (e.g., milli, micro) to the base fluid. However, these experiments did not yield the desired results.

Two decades ago, Choi [10, 11] used nano-sized particles in the base fluid and surprisingly found that the thermal conductivity of nanofluid is significantly greater than that of the base fluid. Following this successful experiment, many theoretical and experimental studies have been conducted to analyze nanofluids, which are now utilized in various thermal engineering processes. For more information on nanofluid, refer to [12-17]. In addition to thermal engineering applications, nanofluids have also shown great promise in biomedical fields. For instance, nanofluids can be used to enhance the thermal conductivity of cancer cells, allowing for more effective thermal ablation treatments. They can also be used as drug delivery agents, with the nanoparticles serving as carriers for targeted drug delivery.

Furthermore, nanofluids can be used to create frameworks for tissue engineering applications, promoting faster healing and tissue growth. Other biomedical applications of nanofluids include medical imaging, wound healing, and biosensing. The unique properties of nanofluids make them an exciting area of research, with potential breakthroughs in various fields, including biomedicine. The Role of

DOI: 10.55214/25768484.v8i6.3147

nanofluids in advancing drug delivery and biomedical innovations was investigated by Sheikhpur et al., [18]. Thermal ablation cancer therapy using nanoparticles and nanomaterials as emerging tools was discovered by Ashikbayeva et al., [19].

A special topic on new improvements of nanofluids related to pharmaceuticals was examined by Ellahi [20]. Medication delivery by ternary Casson hybrid nanofluids in convergent/ divergent channels was probed by Alnahdi et al., [21]. The impact of nanoparticle geometry on peristaltic pumping of medical magnetohydrodynamic nanofluids with energy transfer was studied by Akbar et al., [22]. The flow of MHD hybrid nanoliquid containing medication through a blood artery was inspected by Alghamdi et al., [23].

In many chemical processes, heat and mass transfer occur simultaneously, leading to complex interactions between temperature and concentration gradients. These interactions can cause changes in the concentration of different species in the system. Two important effects to consider in these processes are Soret effect (mass transfer influenced by temperature gradients) and the Dufour effect (heat transfer influenced by concentration gradients).

In biological systems, understanding the coupled transport of heat and mass is crucial, as it can lead to cross-diffusion and changes in concentration gradients of essential species. This is particularly important in processes like metabolic reactions, nutrient uptake, and waste removal. The Soret and Dufour effects, which describe the interplay between heat and mass transfer, have been investigated in various fields, including chemical engineering and geoscience. Similarly, in bio sciences, these effects can play a critical role in understanding phenomena like thermoregulation, blood flow, and nutrient transport. For instance, researchers studying cellular metabolism or tissue engineering may need to consider these effects to optimize their designs and experiments.

Makinde and Olanrewaju [24] examined the effects of Soret and Dufour on unsteady mixed convection flow over a permeable plate moving through a binary mixture of chemically reacting fluid, shedding light on the complex interactions between energy, mass, and momentum transfer in this dynamic system. Hayat et al., [25] conducted a comprehensive investigation into the Soret and Dufour effects on the peristaltic flow of magnetohydrodynamic (MHD) Jeffrey fluid in a rotating system with porous medium.

Mahday [26] studied the energy transfer and liquid flow characteristics of a Casson fluid in the presence of Soret and Dufour effects, which are induced by a stretching cylinder. Srinivasacharya et al., [27] probed the combined impact of Soret and Dufour impects on mixed convection along a vertical surface in a permeable moderate with variable properties. Ahmed et al., [28] research investigated the bioconvective flow of a variable properties hybrid nanoliquid over a rotating disk, examining the combined effects of Arrhenius activation energy, heat and mass transfer and Soret and Dufour impacts on the liquid flow.

Balla et al., [29] explored the combined impact of Soret and Dufour effects on the bioconvective flow of a nanofluid in a porous square cavity. Razaq et al., [30] conducted a study on radiative bioconvective flow with a non-uniform heat source, taking into consideration the effects of Soret and Dufour.

Bio-convection, a fascinating phenomenon where living particles accumulate and form density gradients, has emerged as a vital area of research with far-reaching implications for various industries. Recent discoveries have unveiled the vast potential of bio-convection in biotechnology and biomedical applications, including biofuels, biosensors, drug development, and tissue engineering.

As scientists continue to understand the deep complexities of bio-convection, its significance in understanding complex biological systems and developing innovative solutions for real-world problems becomes increasingly clear. Furthermore, recent breakthroughs in bio-convection research have highlighted its diverse applications and exciting potential for future advancements, paving the way for groundbreaking discoveries and innovative applications that are expected to transform various fields and improve lives. Yin et al., [31] probed the effects of thermal radiation on bioconvection flow of magnetized Sisko nanofluid with swimming microorganisms along a stretching cylinder. Al-Mubaddel et al., [32] studied the double stratification in Sisko nanofluid bioconvection with radiation and generalized fluxes. Puneeth et al., [33] conducted a study on the three-dimensional bioconvective flow of Sisko nanofluid with robin boundary conditions. Raju et al., [34] examined heat and mass transfer in MHD non-Newtonian bio-convection flow over a rotating cone/plate, considering cross diffusion.

This paper studies a new type of fluid flow called bioconvection Sisko nanofluid, which occurs when a stretching cylinder is present and microorganisms are moving around. The fluid's thermal properties are examined under various conditions, including nonlinear thermal radiation and nonuniform heat sources. The analysis additionally takes into account the influences of Soret and Dufour effects. The results are obtained by using a numerical method and graphically presented.

This research is unique and has important implications for various fields, including heat transfer, solar energy, electronics, biofuels, and more. Using MATLAB software Bvp4c solver, we've generated numerical results that shed light on the crucial role of key physical parameters. Remarkably, this innovative flow model boasts unique thermal properties that have never been explored before, making it a pioneering achievement. Our discoveries have significant implications for various bio sciences applications, including bioprocessing, biomedical devices, bioelectronics, biofuels, enzyme technology, and biomedical research.

2. Description of the Problem

This study examined the 2D, incompressible, steady flow of Sisko nanofluid past a stretching cylinder. To expand the study's range, Soret and Dufour effects are incorporated into the analysis. A transverse magnetic field of strength B_0 is applied perpendicularly to the surface of the cylinder, in the radial direction (along the r direction) as shown in Figure 2.

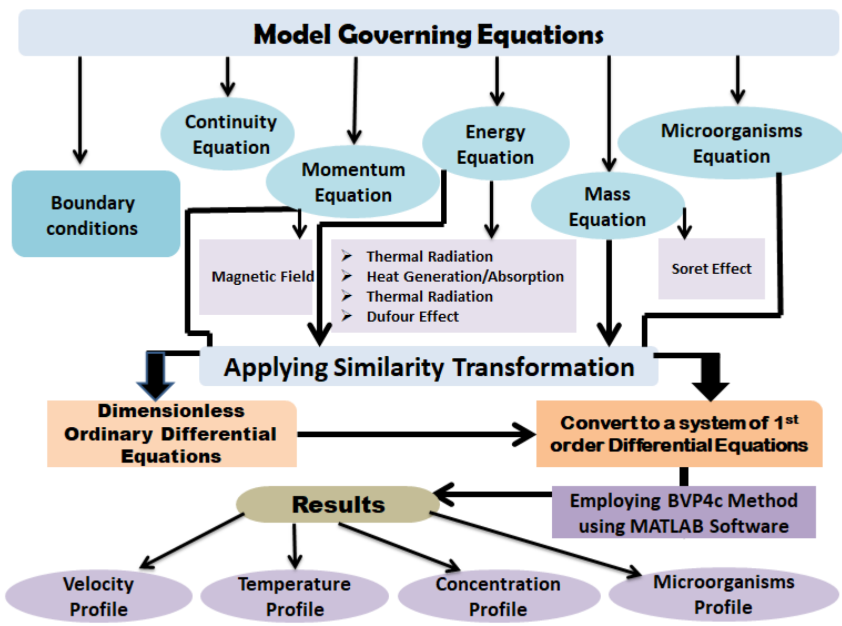

Figure 2.
Diagrammatic representation of the mathematical model using BVP4c.

The Sisko nanofluid is assumed to be continuous in nature, and its physical properties are uninterrupted. Furthermore, the effect of viscous dissipation is neglected in this analysis. Figure 3 shows a schematic representation of the flow problem and the associated coordinate system.

ISSN: 2576-8484
Vol. 8, No. 6: 5236-5253, 2024
DOI: 10.55214/25768484.v8i6.3147

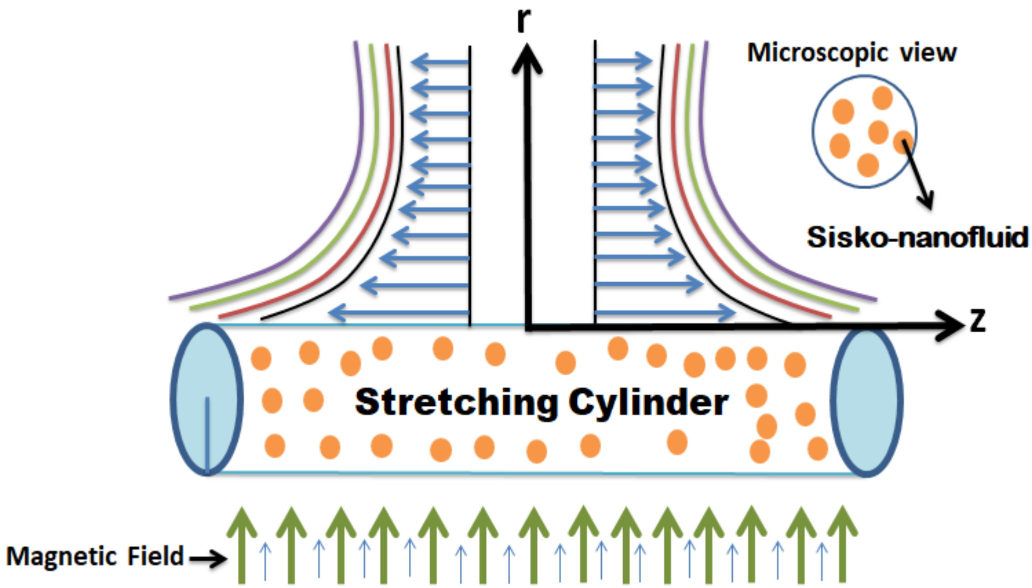

Figure 3.
Geometrical layout.

Under the above assumptions, the governing equations for 2D Sisko nanofluid flow through swimming microorganisms on a stretching surface, as described in references [35-36], can be written as follows:

$$\frac{\partial ru}{\partial x}+\frac{\partial rv}{\partial r}=0, \tag{1}$$

$$u\frac{\partial u}{\partial x}+v\frac{\partial v}{\partial r}=\frac{a_1}{\rho_{nf}}\frac{\partial}{\partial r}\left(r\frac{\partial u}{\partial r}\right)-\frac{a_2}{r\rho_{nf}}\left(-\frac{\partial u}{\partial r}\right)^m+\frac{ma_2}{\rho_{nf}}\left(-\frac{\partial u}{\partial r}\right)^{m-1}\frac{\partial u^2}{\partial^2 r}-\frac{\varepsilon v}{K_p}u+$$
$$\frac{1}{\rho_{nf}}\left[(1-C_\infty)\rho_{nf}\beta^* g(T-T_\infty)-\left(\rho_{np}-\rho_{nf}\right)g(C-C_\infty)-(N-N_\infty)g\gamma^*\left(\rho_{nm}-\rho_{nf}\right)\right], \tag{2}$$

$$u\frac{\partial T}{\partial x}+v\frac{\partial T}{\partial r}=\frac{1}{r}\frac{\partial}{\partial r}\left(ar\frac{\partial T}{\partial r}\right)+\tau\left[D_B\frac{\partial C}{\partial r}\frac{\partial T}{\partial r}+\frac{D_T}{T_\infty}\left(\frac{\partial T}{\partial r}\right)^2\right]+\frac{Q_0}{\rho_f c_{pf}}(T-T_\infty)+$$
$$\frac{{Q_0}^*}{\rho_f c_{pf}}(T_w-T_\infty)exp\left(-n\left(\frac{2Rx}{r^2-R^2}\,\frac{1}{Re_{a_2}^{\frac{1}{(m+1)}}}\right)\right)+\frac{1}{(\rho c)_f}\frac{\partial\left(r\frac{16}{3}\frac{\sigma^* T_\infty^3}{k^*}\frac{\partial T}{\partial r}\right)}{\partial r}+\frac{D_T K_T}{C_s C_p}\frac{\partial^2 C}{\partial r^2}, \tag{3}$$

$$u\frac{\partial C}{\partial x}+v\frac{\partial C}{\partial r}=D_B\frac{\partial^2 C}{\partial r^2}+\frac{D_T K_T}{T_\infty}\frac{\partial^2 T}{\partial r^2}, \tag{4}$$

$$u\frac{\partial N}{\partial x}+v\frac{\partial N}{\partial r}+\frac{bW_c}{(C_w-C_\infty)}\left[\frac{\partial}{\partial r}\left(N\frac{\partial C}{\partial r}\right)\right]=D_m\left(\frac{\partial^2 N}{\partial r^2}\right), \tag{5}$$

The problem is subject to the following boundary conditions:

$$u=cx+\frac{\beta^*}{r}\frac{\partial u}{\partial r},\ v=0,\ -k\frac{\partial T}{\partial r}=h_f(T_w-T),$$
$$-D_B\frac{\partial C}{\partial r}=h_g(C_w-C),\ -D_m\frac{\partial N}{\partial r}=h_n(N_w-N)\quad \text{at}\quad r=0 \tag{6}$$
$$u\to 0,\ \ N\to 0,\ \ T\to T_\infty,\ \ C\to C_\infty,\ N\to N_\infty \qquad \text{as} \qquad r\to\infty \tag{7}$$

The material constants for the Sisko fluid represent the following physical properties and parameters:

ISSN: 2576-8484
Vol. 8, No. 6: 5236-5253, 2024
DOI: 10.55214/25768484.v8i6.3147

Table 1.

a_1	Viscosity at an extremely high shear rate
a_2	Consistency index or viscosity in the power-law region
m	Power-law index, which varies depending on the specific fluid
ρ_{nf}	Density of Sisko nanofluid
v	Density
ρ_f	Density of fluid
ρ_{nm}	Density of nano microorganisms
ρ_{np}	Density of nanoparticles
β^*	Volume expansion coefficient
γ^*	Average volume of microorganisms
T	Temperature
$T\infty$	ambient temperature
C	Concentration
C_∞	Ambient concentration
N	Microorganisms
N_∞	Ambient microorganisms
$(\rho c)_f$	Heat capacity of the base fluid
g	Gravitational acceleration
τ	Parameter defined by the ratio $\frac{(\rho c)_p}{(\rho c)_f}$
D_B	Brownian motion
D_T	Thermophoresis diffusion coefficient
Q_0	Heat generation/ absorption parameter
c_{nf}	Specific heat of nanofluid
σ^*	Stefan–Boltzmann constant
k^*	Thermal conductivity
b	Chemotaxis constant
W_c	Maximum speed of swimming
B^*	Porosity parameter
k	Thermal conductivity
h_f	Convection heat transport
N_w	Wall microorganism
D_m	Diffusion coefficient of microorganisms

The current problem's convergence to nonlinear dimensionless ODEs is similar.

$$\zeta = \frac{r^2-R^2}{2Rx}\, Re_{a_2}^{1/(m+1)}, f(\zeta) = \psi\, \frac{1}{RxU_w Re_{a_2}^{-1/(m+1)}},$$
$$\theta(\zeta) = \frac{T-T_\infty}{T_w-T_\infty}, \phi(\zeta) = \frac{C-C_\infty}{C_w-C_\infty}, \chi(\zeta) = \frac{N-N_\infty}{N_w-N_\infty}, \tag{8}$$

The function of the velocity stream is:

$$u = \frac{\partial\psi}{\partial r}, v = -\frac{\partial\psi}{\partial x} \tag{9}$$

ISSN: 2576-8484
Vol. 8, No. 6: 5236-5253, 2024
DOI: 10.55214/25768484.v8i6.3147

The system of coupled partial differential equations (1-5) with boundary conditions (6-7) is reduced to a set of nonlinear dimensionless ordinary differential equations (ODEs) through the similarity transformations (8).

$$B(1+2\alpha\zeta)f''' + m(-f'')^{m-1}(1+2\alpha\zeta)^{\frac{m+1}{2}}f''' + 2\alpha Bf'' + \frac{2m}{m+1}ff'' - (f')^2 - Mf' - (-f'')^m(1+m)(1+2\alpha\zeta)^{\frac{m+1}{2}} + \beta(\theta - Nr\phi - Nc\chi) = 0 \quad (10)$$

$$(1+2\alpha\zeta)\theta'' + 2\alpha\theta' + \left[\{1 + Rd(1+(\theta_f - 1)\theta)^3\}(1+2\alpha\zeta)\theta'\right]\theta'' + Pr\left(\frac{2m}{m+1}\right)f\theta' + (1+2\alpha\zeta)\,\mathrm{Pr}(Nb\theta'\phi' + Nt(\theta')^2) + PrQ_p\theta + PrQ_E\exp(-n\zeta) + DfPr\phi'' = 0, \quad (11)$$

$$(1+2\alpha\zeta)\phi'' + 2\alpha\phi' + \frac{Nt}{Nb}2\alpha\theta'' + (1+2\alpha\zeta)Lb\,Sr\theta'' + LePr\left(\frac{2m}{m+1}\right)f\phi' = 0, \quad (12)$$

$$(1+2\alpha\zeta)\chi'' + 2\alpha\chi' + Lb\left[\left(\frac{2m}{m+1}\right)(f\chi')\right] - Pe[\phi''(\chi + \Omega_1) + \chi'\phi'] = 0, \quad (13)$$

With associated boundary conditions

$$f(0) = 0, f'(0) = 1 + \lambda f''(0), \theta'(0) = -A_1(1-\theta(0)),$$
$$\phi'(0) = -A_2(1-\phi(0)),\ \chi'(0) = -A_3(1-\chi(0)), \quad (14)$$
$$f'(\infty) \to 0, \theta(\infty) \to 0, \phi(\infty) \to 0, \chi(\infty) \to 0,$$

The physical system is characterized by a set of dimensionless parameters, including the material parameter, mixed convection parameter, buoyancy ratio parameter, bioconvection Rayleigh number, radiation parameter, temperature ratio parameter, Prandtl number , local Reynolds numbers, thermal dependent heat source parameter, exponential space based source parameter, curvature parameter, thermophoresis parameter, magnetic parameter, Brownian motion parameter, Lewis number, bioconvection Lewis number, Peclet number, thermal Biot number, solutal Biot number, microorganisms Biot number, velocity slip parameter, Soret and Dufour effect parameters. These parameters are used to nondimensionalize the governing equations and boundary conditions, allowing for a more concise and meaningful analysis of the system's behavior.

$$B = \frac{Re_{a_2}^{\frac{2}{(m+1)}}}{Re_{a_1}},\quad \beta = \frac{c(1-C_f)(T_f - T_\infty)\beta^* g^*}{x},\quad Nr = \frac{(\rho_p - \rho_f)(C_f - C_\infty)}{\beta^*(1-C_f)(T_f - T_\infty)\rho_f},\ Nc = \frac{(\rho_m - \rho_f)(N_f - N_\infty)\gamma^{**}Q_p}{\beta^*(1-C_f)(T_f - T_\infty)\rho_f},\quad Rd = \frac{16\sigma^* T_\infty^3}{3kk^*},\quad Pr = \frac{xU_x}{\alpha}Re_{a_2}^{\frac{2}{(m+1)}}, Re_{a_1} = \frac{\rho_{nf}U_w x}{a_1},\quad Re_{a_2} = \frac{\rho_{nf}x^m U_w^{2-m}}{a_2},\ Q_p = \frac{Q_0}{\rho_f C_{pf}},$$
$$Q_E = \frac{Q_0^*}{\rho_f C_{pf}},\quad \alpha = \frac{x}{R}Re_{a_2}^{\frac{2}{(m+1)}},\quad Nt = \frac{\tau D_T(T_w - T_\infty)}{\alpha T_\infty},\quad M = \frac{v\varepsilon x}{K_p U_w},\quad Nb = \frac{\tau D_B(C_w - C_\infty)}{\alpha}, Le = \frac{\alpha}{D_B},\quad Lb = \frac{v}{D_m},$$
$$Pe = \frac{bW_e}{D_m},\ A_1 = \frac{xRh_f}{kRe_b^{-\frac{1}{m+1}}},\ A_2 = \frac{xRh_g}{D_B Re_b^{-\frac{1}{m+1}}},\ A_3 = \frac{xRh_n}{D_m Re_b^{-\frac{1}{m+1}}},\ \lambda = \frac{\beta^*}{xRRe_b^{-\frac{1}{m+1}}},$$
$$Sr = \frac{D_T K_T}{T_\infty \vartheta}\frac{(T_w - T_\infty)}{(C_w - C_\infty)},\ Dr = \frac{D_T K_T}{C_p C_s}\frac{(C_w - C_\infty)}{v(T_w - T_\infty)}, \quad (15)$$

The important engineering values, such as the dimensional Nusselt number N_{u_x} and heat transfer rate is given as:

$$Nu_x = \frac{xq_w}{k(T_w - T_\infty)}, \quad (16)$$

Herer $q_w = -k\left(\frac{\partial T}{\partial r}\right)_{r=0}$ is heat flux.

The non-dimensional form is

$$Nu_x Re_{a_2}^{-\frac{1}{m+1}} = -\theta'(0). \quad (17)$$

3. Numerical Method

In this section, we investigate the bio-convection effects of Sisko nanoliquid flow above an extending cylinder, taking into consideration the Soret and Dufour effects. We numerically solve the coupled nonlinear differential equations (10-13) with boundary conditions (14) using the built-in MATLAB function bvp4c. This solver utilizes a finite difference method to convert the fourth-order differential equations into linear form. To implement this solver, we rewrite the higher-order differential equations as a system of first-order differential equations by introducing auxiliary variables, as shown below.

Step 1: For the following coupled nonlinear ODEs, add new parameters:

$$y(1) = f, y(2) = f', y(3) = f'', y'(3) = f''', y(4) = \theta, y(5) = \theta', y'(5) = \theta''$$
$$y(6) = \phi, y(7) = \phi', y'(7) = \phi''\ y(8) = \chi, y(9) = \chi', y'(9) = \chi''$$

Step 2: The following parameters of step 1 should be written into the 1st order system of equations:

$$y(1) = f, \qquad y(2) = f', \qquad y(3) = f''$$

$$y'(3) = \frac{(y(2))^2 + My(2) - \left(-y(3)\right)^m (1+m)(1+2\alpha\zeta)^{\frac{m+1}{2}} - \beta(\theta - Nry(6) - Ncy(8)) - 2\alpha By(3) - \frac{2m}{m+1}y(1)y(3)}{\left[B(1+2\alpha\zeta) + m(-y(3))^{m-1}(1+2\alpha\zeta)^{\frac{m+1}{2}}\right]} \tag{18}$$

$$y(4) = \theta \ , \quad y(5) = \theta'$$

$$y'(5) = \frac{-\left[Pr\left(\frac{2m}{m+1}\right)y(1)y(5) + (1+2\alpha\xi)\Pr\left(Nby(5)y(7) + Nt(y(5))^2\right) + PrQ_p y(4) + PrQ_E \exp(-\eta\zeta) - 2\alpha y(5) + DfPry'(7)\right]}{(1+2\alpha\zeta) + \left[\left\{1 + Rd\left(1 + (\theta_f - 1)y(4)\right)^3\right\}(1+2\alpha\zeta)y(5)\right]}$$

(19)

$$y(6) = \phi, \qquad y(7) = \phi$$

$$y'(7) = \frac{-\left[2\alpha y(7) + \left\{\frac{Nt}{Nb}2\alpha + (1+2\alpha\zeta)Lb\ Sr\right\}y'(5) + LePr\left(\frac{2m}{m+1}\right)y(1)y(7)\right]}{(1+2\alpha\zeta)} \tag{20}$$

$$y(8) = \chi \ , \qquad y(9) = \chi'$$

$$y'(9) = \frac{Pe\left[y'(7)(y(8) + \Omega_1) + y(9)y(7)\right] - Lb\left[\left(\frac{2m}{m+1}\right)\left(y(1)y(9)\right)\right] - 2\alpha\ y(9)}{(1+2\alpha\zeta)} \tag{21}$$

Step 3: The boundary conditions of (6-7) are rewritten in the term of new variable as:

$$ya(1) = 0,\ ya(2) = 1 + \lambda\ \ ya(3), ya(3) = -A_1(1 - ya(4)),$$
$$ya(7) = -A_2(1 - ya(6)), ya(9) = -A_3(1 - ya(8)) \tag{22}$$
$$yb(2) \to 0, yb(4) \to 0, yb(6) \to 0, yb(8) \to 0$$

Consequently, the variable a represents the conditions on the sheet, which is denoted by $\xi = 0$, and the variable b represents the conditions off the sheet, for example, $\xi = 1$.

Step 4: In MATLAB, use the bvp4c solver to solve the system of first-order ODEs (18-21) with boundary conditions (22).

4. Results and Discussion

This section provides a numerical analysis of various engineering quantities in response to changes in different parameters. By solving the governing differential equations numerically, we gain flexibility in selecting suitable flow parameter values and a deeper understanding of the physical problem. The results are presented in tables as follows: Table 2 shows the numerical results for local skin friction coefficients, while Table 3 provides the local Nusselt numbers, Table 4 compares the Sherwood numbers across different parameters, and Table 5 details the density of local microorganisms.

Additionally, we have graphically examined the impects of Magnetic parameter M, buoyancy ratio factor Nr, mixed convection parameter β, thermal Biot number A_1, Dufour effect parameter Df,

Edelweiss Applied Science and Technology
ISSN: 2576-8484
Vol. 8, No. 6: 5236-5253, 2024
DOI: 10.55214/25768484.v8i6.3147

Prandtl number Pr, Brownian motion factor Nb, Soret effect parameter Sr, microorganisms Biot number A_3 and Peclet number Pe on velocity, temperature, concentration and microorganism profiles. All graphical findings were developed using the properties of shear-thinning $(m < 1)$ and shear-thickening $(m > 1)$ fluids, which are effectively represented by the Sisko fluid model.

These tables provide a complete summary of the numerical results, highlighting the impacts of different parameters on the engineering quantities.

Table 2.
Numerical analysis of local skin friction coefficient using different parameter values.

M	β	Nr	Nc	B	α	$-[Bf''(0) - \{f''(0)\}^{\frac{1}{2}}]$	$-(B+1)f''(0)$	$-[Bf''(0) - f''^2(0)]$
0.5	0.2	0.2	0.2	0.5	0.2	0.4712	0.9565	0.0987
0.7						0.4722	1.0001	0.1102
1.3						0.4856	1.0211	0.1214
	0.7					0.4771	0.9368	0.0787
	1.2					0.4753	0.8956	0.0475
	1.7					0.4614	0.8576	0.0425
		0.7				0.4992	0.9987	0.1141
		1.4				0.4959	1.1101	0.1260
		2.5				0.4978	1.1365	0.1412
			0.7			0.4806	0.9835	0.1045
			1.4			0.4832	1.0314	0.1278
			2.5			0.4878	1.0510	0.1393
				0.2		0.4772	0.9612	0.0865
				0.5		0.4821	0.9765	0.09989
				0.9		0.4845	1.0042	0.1132
					0.5	0.4841	1.0096	0.1121
					0.9	0.4887	1.0662	0.1496
					1.3	0.4914	1.1164	0.1823

Table 3.
Numerical analysis of local Nusselt number using different parameter values.

Parameters							$-\theta'(0)$	
Pr	Nt	Rd	Nr	Nc	λ	Q_E	$m = 0.5$	$m = 2.0$
2.5	0.3	0.5	0.1	0.1	1.0	0.3	0.1922	0.1897
3.5							0.1966	0.1935
4.5							0.2001	0.1966
2.0	0.1						0.1935	0.1914
	0.4						0.1876	0.1853
	0.8						0.1791	0.1766
		1.0					0.1742	0.1719
		1.5					0.1626	0.1604
		2.0					0.1536	0.1516
			0.5				0.1889	0.1756
			2.0				0.1854	0.1607
			3.5				0.1803	0.1521
				0.5			0.1877	0.1762
				2.0			0.1851	0.1734
				3.5			0.1801	0.1791
					2.0		0.1829	0.1809

					3.0		0.1794	0.1777
					4.0		0.1773	0.1757
						0.5	0.1887	0.1760
						1.2	0.1765	0.1678
						2.4	0.1753	0.1597

Table 4.
Numerical analysis of Sherwood number using different parameter values.

Parameters								$-\phi'(0)$	
Pr	Nt	Nb	Nr	Nc	λ	Le	A_2	$m = 0.5$	$m = 2.0$
2.4	0.3	0.2	0.1	0.1	1.0	2.0	0.4	0.2702	0.2676
3.4								0.2852	0.2835
4.4								0.2965	0.2946
2.0	0.15							0.2851	0.1905
	0.45							0.2464	0.1842
	0.85							0.2045	0.1764
		0.2						0.2703	0.2712
		0.4						0.2864	0.2854
		0.6						0.2924	0.2806
			0.4					0.2571	0.2574
			1.9					0.2545	0.2548
			3.4					0.2536	0.2527
				0.3				0.2576	0.2548
				1.8				0.2547	0.2538
				3.3				0.2539	0.2528
					1.5			0.2538	0.2521
					2.5			0.2509	0.2504
					3.5			0.2500	0.2478
						2.5		0.2804	0.2778
						3.5		0.2937	0.2919
						4.5		0.3032	0.3021
							0.5	0.4748	0.4663
							1.0	0.5818	0.5744
							1.5	0.6562	0.6463

Table 5.
Numerical analysis of local microorganism density number using different parameter values.

Parameters						$-\chi'(0)$	
Pe	Lb	Nr	Nc	λ	A_3	$m = 0.5$	$m = 2.0$
0.5	2.0	0.1	0.1	1.0	0.4	0.2024	0.1954
1.2						0.2398	0.2340
1.3						0.2654	0.2627
0.1	2.5					0.2232	0.2154
	4.0					0.2502	0.2432
	5.0					0.2656	0.2582
		0.3				0.1912	0.1904
		1.5				0.1800	0.1778
		3.0				0.1598	0.1582
			0.3			0.1875	0.1865
			1.5			0.1865	0.1856
			3.0			0.1802	0.1808

				1.5		0.1735	0.1658
				2.5		0.1612	0.1545
				3.5		0.1547	0.1485
					1.5	0.2753	0.2701
					2.0	0.3132	0.2910
					2.5	0.3216	0.3098

Figure 4 shows the impact of magnetic parameter M on velocity profile for both conditions shear-thinning and shear-thickening fluids $(m = 0.5\ and\ m = 2.0)$. The Sisko fluid's velocity decreases with increasing magnetic parameter. Growing values of the magnetic parameter reduce the fluid's velocity by acting as a resistive force in the flow known as the Lorentz force. From a physical perspective, the magnetic parameter affects the Lorentz force, which defines the characteristics of fluid motion in the flow system.

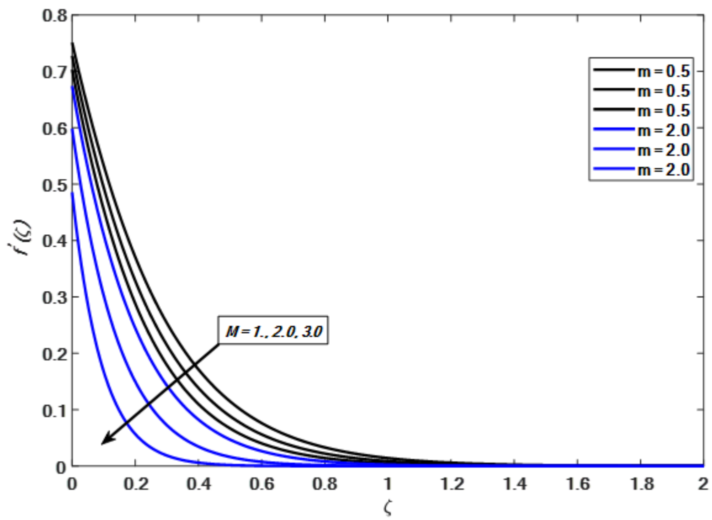

Figure 4.
Variation in $f'(\varsigma)$ with M at shear rates $m = 0.5$ and $m = 2.0$.

Figure 5 illustrates the impact of the buoyancy ratio factor Nr on the velocity profile for both shear-thinning and shear-thickening fluids $(m = 0.5\ and\ m = 2.0)$.The Sisko fluid velocity decreases as the values of the buoyancy ratio parameter Nr increase.

ISSN: 2576-8484
Vol. 8, No. 6: 5236-5253, 2024
DOI: 10.55214/25768484.v8i6.3147

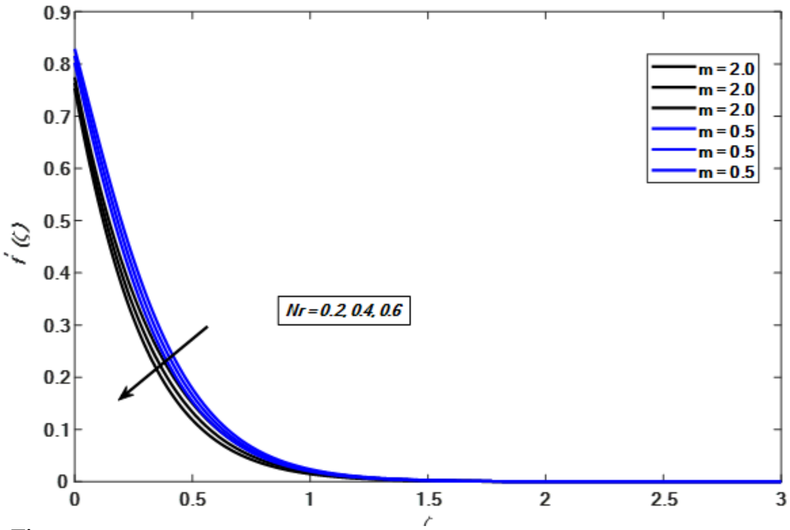

Figure 5.
Variation in $f'(\varsigma)$ with Nr at shear rates $m = 0.5$ and $m = 2.0$.

Figure 6 demonstrates the effect of the mixed convection parameter β on the velocity field, showing that an increase in this parameter improves the velocity field for both values ($m = 0.5$ *and* $m = 2.0$).

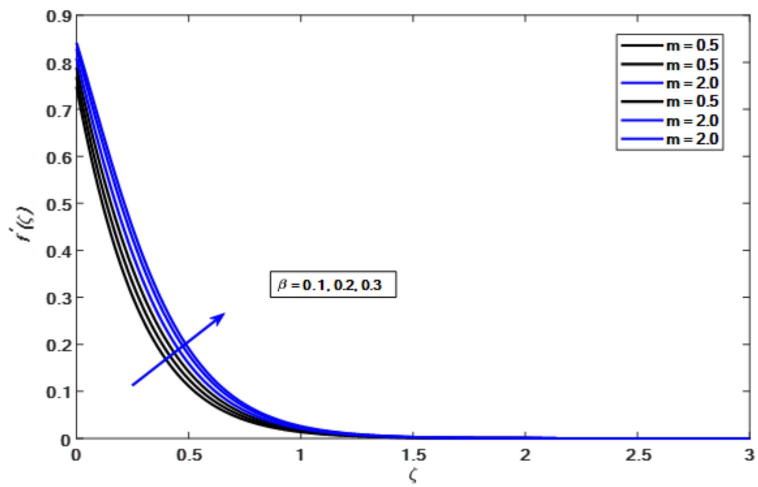

Figure 6.
Variation in $f'(\varsigma)$ with β at shear rates $m = 0.5$ and $m = 2.0$.

Figure 7 depicts the effect of the thermal stratification Biot number A_1 on temperature distribution. It is shown that both shear-thinning and shear-thickening fluids (*m=0.5 and m=2.0*) have a better temperature distribution when the thermal stratification Biot number rises.

Edelweiss Applied Science and Technology
ISSN: 2576-8484
Vol. 8, No. 6: 5236-5253, 2024
DOI: 10.55214/25768484.v8i6.3147

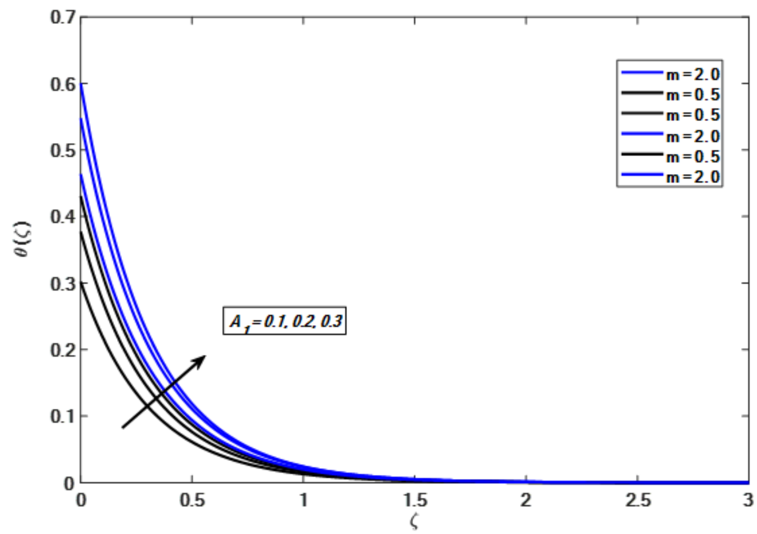

Figure 7.
Variation in $\theta(\varsigma)$ with A_1 at shear rates $m = 0.5$ and $m = 2.0$.

Figure 8 represents the behaviour of Dufour effect parameter Df on temperature profile for both cases $(m = 0.5\ and\ m = 2.0)$.Higher Dufour effect parameter boosts the energy flux caused by concentration differences. This effect is most noticeable when irreversible processes are present, leading to changes in the temperature profile due to variations in concentration.

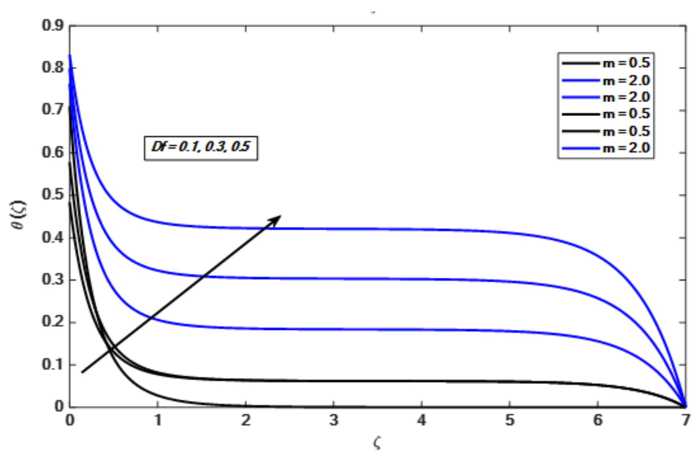

Figure 8.
Variation in $\theta(\varsigma)$ with Df at shear rates $m = 0.5$ and $m = 2.0$.

Figure 9 signifies the features of Brownian motion parameter Nb on the temperature profile for both shear-thinning and shear-thickening fluids $(m = 0.5\ and\ m = 2.0)$. As the Brownian motion parameter Nb increases, the random motion of fluid particles intensifies, leading to greater layer thickness. Brownian motion, which refers to the random movement of suspended particles in a fluid, causes the temperature of the Sisko fluid to rise due to interaction between these particles. This results in an enhanced temperature profile.

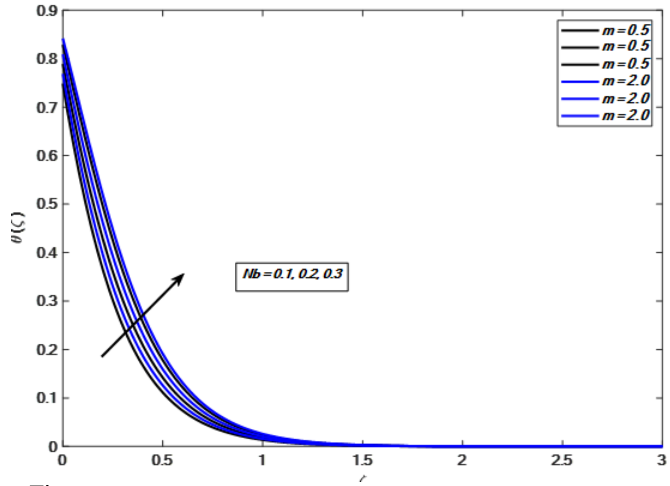

Figure 9.
Variation in $\theta(\varsigma)$ with Nb at shear rates $m = 0.5$ and $m = 2.0$.

Figure 10 examine the behaviour of Prandtl number Pr on the concentration profile for both shear-thinning and shear-thickening fluids $(m = 0.5\ and\ m = 2.0)$. It is observed that the concentration distribution decreases as the Prandtl number increases in both types of fluids.

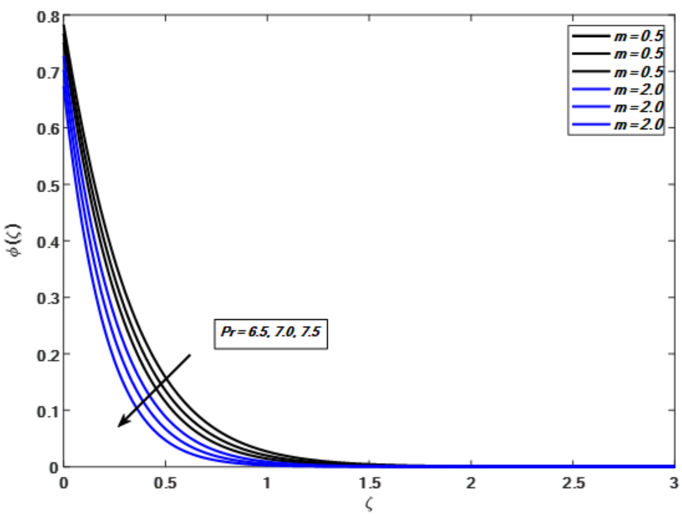

Figure 10.
Variation in $\phi(\varsigma)$ with Pr at shear rates $m = 0.5$ and $m = 2.0$.

Figure 11 shows the Soret effect parameter Sr on the concentration profile for both cases $(m = 0.5\ and\ m = 2.0)$. The concentration profile turns up for higher values of Sr, because mass flux caused by temperature differences.

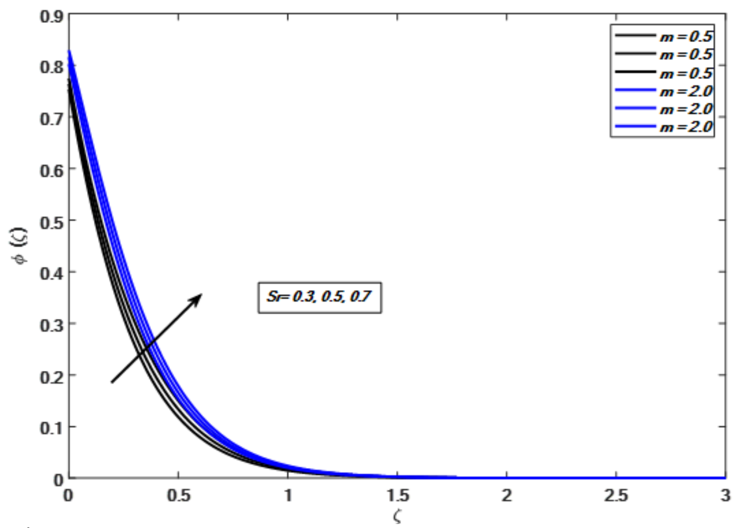

Figure 11.
Variation in $\phi(\varsigma)$ with Sr at shear rates $m = 0.5$ and $m = 2.0$.

Figure 12 reflect the results of the Biot number of microorganism stratification A_3 on the microorganism concentration field for both shear-thinning and shear-thickening fluids $(m = 0.5\ and\ m = 2.0)$. The findings indicate that when the microorganism stratification Biot number increases, the microorganism concentration field becomes progressively more significant.

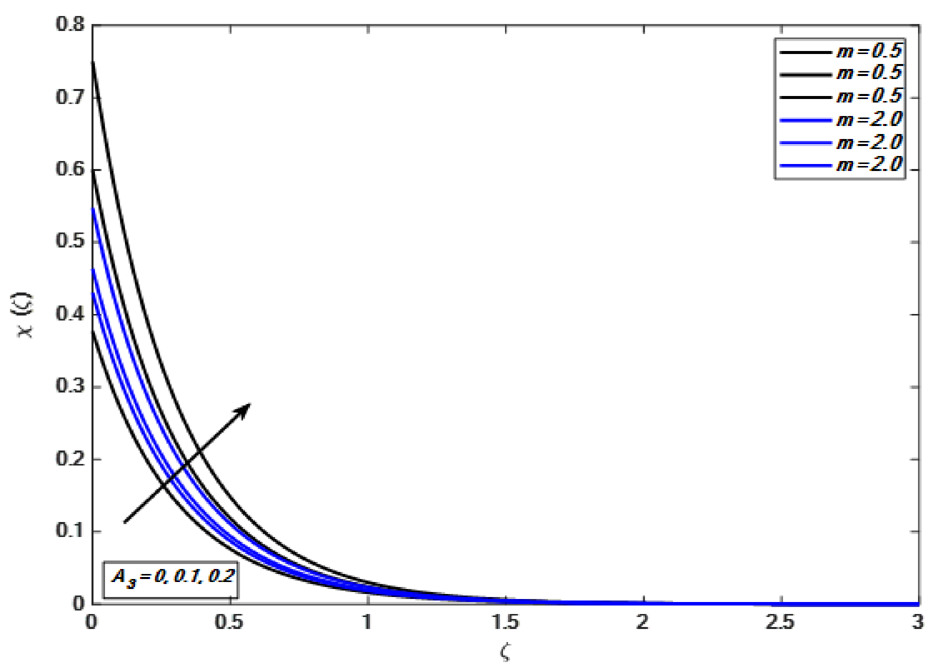

Figure 12.
Variation in $\chi(\varsigma)$ with A_3 at shear rates $m = 0.5$ and $m = 2.0$.

Figure 13 sketch to examine the nature of Peclet number Pe on the microorganism's concentration of nanoparticles. The graph shows that increased Peclet number leads to decrease the dispersion of microorganisms in both shear-thinning and shear-thickening fluids.

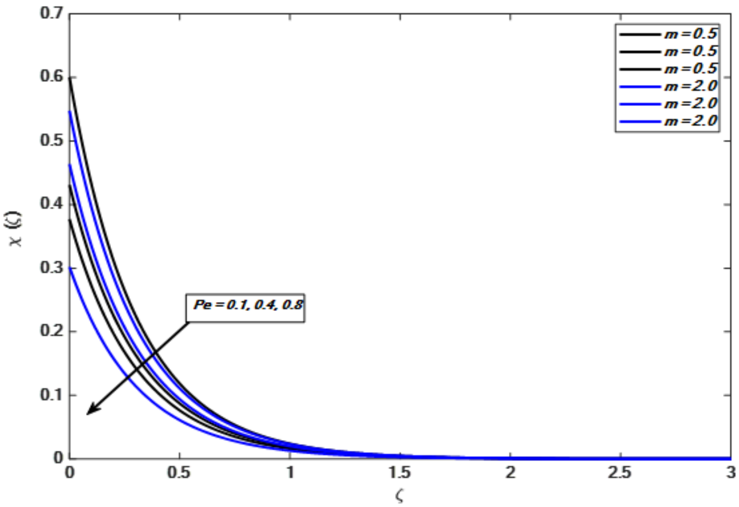

Figure 13.
Variation in $\chi(\varsigma)$ with Pe at shear rates $m = 0.5$ and $m = 2.0$.

5. Conclusion

This research explores the bio-convection flow of Sisko nanofluid containing microorganisms over a stretchy cylinder, taking into account Soret and Dufour effects. Bvp4c method is utilized to attain numerical results. The Buongiorno model is used to examine thermophoresis and Brownian motion factors. Main findings are:

1. Velocity profile declines as the magnetic parameter rises.
2. Velocity profile decreases with increasing values of buoyancy ratio factor and mixed convection parameter.
3. Temperature profile boosts with higher Biot number, Dufour parameter and Brownian motion factor.
4. Concentration profile turns up as the Prandtl number and Soret effect parameter increase.
5. Microorganisms profile expands with higher values of microorganisms Biot number while contradictory behaviour is noticed for Peclet number.

Acknowledgement:

The authors extend their appreciation to the Arab Open University for funding this work through AOU research fund No. (AOURG-2023-016).

References

[1] Adesanya, S. O., Adeosun, A. T., Lebelo, R. S., & Tisdell, C. C. (2024). Numerical investigation of reaction driven magneto-convective flow of Sisko fluid. *Numerical Heat Transfer, Part A: Applications*, 1-14.

[2] Hafez, N. M. (2024). EHD peristaltic flow of Sisko fluid under the effects of convection and endoscope. *Ain Shams Engineering Journal*, *15*(5), 102647.

[3] Islam, T., Ferdows, M., Shamshuddin, M. D., Alqarni, M. S., & Usman. (2024). Sisko fluid modeling and numerical convective heat transport analysis over-stretching device with radiation and heat dissipation. *Numerical Heat Transfer, Part A: Applications*, *85*(8), 1240-1258.

[4] Khan, M., Abelman, S., Mason, D. P., & Mahomed, F. M. (2015). Self-similar unsteady flow of a Sisko fluid in a cylindrical tube undergoing translation. *Mathematical Problems in Engineering*, *2015*.

[5] Nisha, S. S., & De, P. (2024). Impact of electro-osmotic, activation energy and chemical reaction on Sisko fluid over Darcy–Forchheimer porous stretching cylinder. *Proceedings of the Institution of Mechanical Engineers, Part E: Journal of Process Mechanical Engineering*, 09544089241255657.
[6] Prasannakumara, B. C., Gireesha, B. J., Krishnamurthy, M. R., & Kumar, K. G. (2017). MHD flow and nonlinear radiative heat transfer of Sisko nanofluid over a nonlinear stretching sheet. *Informatics in Medicine Unlocked*, *9*, 123-132.
[7] Upreti, H., Joshi, N., Pandey, A. K., & Rawat, S. K. (2022). Assessment of convective heat transfer in Sisko fluid flow via stretching surface due to viscous dissipation and suction. *Nanoscience and Technology: An International Journal*, *13*(2).
[8] Imran, N., Javed, M., Sohail, M., Gokul, K. C., & Roy, P. (2020). Exploration of thermal transport for Sisko fluid model under peristaltic phenomenon. *Journal of Physics Communications*, *4*(6), 065003.
[9] Bisht, A., & Bisht, A. S. (2022). Radiative heat transfer due to solar radiation in MHD Sisko nanofluid flow. *Heat Transfer*, *51*(8), 7411-7434.
[10] Choi, S. U., & Eastman, J. A. (1995). *Enhancing thermal conductivity of fluids with nanoparticles* (No. ANL/MSD/CP-84938; CONF-951135-29). Argonne National Lab.(ANL), Argonne, IL (United States).
[11] Choi, S. U. S., Zhang, Z. G., Yu, W., Lockwood, F. E., & Grulke, E. A. (2001). Anomalous thermal conductivity enhancement in nanotube suspensions. *Applied physics letters*, *79*(14), 2252-2254.
[12] Bouchireb, A., Khan, I., Kezzar, M., Alqahtani, S., Sari, M. R., Rafique, K., & Tabet, I. (2024). MHD Flow of Hybrid Nanofluid Between Convergent/Divergent Channel by Using Daftardar-Jafari Method. *BioNanoScience*, 1-18.
[13] Rafique, K., Alqahtani, A. M., Ahmad, S., Alotaibi, H., Khan, I., & Singh, A. (2024). Buongiorno Model of Micropolar Nanofluid with Surface Inclination and Soret Effect. *BioNanoScience*, 1-11.
[14] Lemouedda, B., Kezzar, M., Rafique, K., Sari, M. R., Tabet, I., & Khan, I. (2024). Ternary nanoparticles effect in rotating hydromagnetic Jeffery-Hamel flow of nanofluids. *Proceedings of the Institution of Mechanical Engineers, Part N: Journal of Nanomaterials, Nanoengineering and Nanosystems*, 23977914241261514.
[15] Al Faqih, F. M., Rafique, K., Aslam, S., & Swalmeh, M. Z. (2024). Numerical Analysis on Stagnation Point Flow of Micropolar Nanofluid with Thermal Radiations over an Exponentially Stretching Surface. *WSEAS Transactions on Fluid Mechanics*, *19*, 40-48.
[16] Ali, A. R., Rafique, K., Imtiaz, M., Jan, R., Alotaibi, H., & Mekawy, I. (2024). Exploring magnetic and thermal effects on MHD bio-viscosity flow at the lower stagnation point of a solid sphere using Keller box technique. *Partial Differential Equations in Applied Mathematics*, *9*, 100601.
[17] Alotaibi, H., & Rafique, K. (2022). Numerical simulation of nanofluid flow between two parallel disks using 3-stage Lobatto III-A formula. *Open Physics*, *20*(1), 649-656.
[18] Sheikhpour, M., Arabi, M., Kasaeian, A., Rokn Rabei, A., & Taherian, Z. (2020). Role of nanofluids in drug delivery and biomedical technology: Methods and applications. *Nanotechnology, Science and Applications*, 47-59.
[19] Ashikbayeva, Z., Tosi, D., Balmassov, D., Schena, E., Saccomandi, P., & Inglezakis, V. (2019). Application of nanoparticles and nanomaterials in thermal ablation therapy of cancer. *Nanomaterials*, *9*(9), 1195.
[20] Ellahi, R. (2018). Special issue on recent developments of nanofluids. *Applied Sciences*, *8*(2), 192.
[21] Alnahdi, A. S., Nasir, S., & Gul, T. (2023). Ternary Casson hybrid nanofluids in convergent/divergent channel for the application of medication. *Thermal Science*, *27*(Spec. issue 1), 67-76.
[22] Akbar, N. S., Tripathi, D., & Bég, O. A. (2016). Modeling nanoparticle geometry effects on peristaltic pumping of medical magnetohydrodynamic nanofluids with heat transfer. *Journal of Mechanics in Medicine and Biology*, *16*(06), 1650088.
[23] Alghamdi, W., Alsubie, A., Kumam, P., Saeed, A., & Gul, T. (2021). MHD hybrid nanofluid flow comprising the medication through a blood artery. *Scientific Reports*, *11*(1), 11621.
[24] Makinde, O. D., & Olanrewaju, P. O. (2011). Unsteady mixed convection with Soret and Dufour effects past a porous plate moving through a binary mixture of chemically reacting fluid. *Chemical Engineering Communications*, *198*(7), 920-938.
[25] Hayat, T., Rafiq, M., & Ahmad, B. (2016). Soret and Dufour effects on MHD peristaltic flow of Jeffrey fluid in a rotating system with porous medium. *PloS one*, *11*(1), e0145525.
[26] Mahdy, A. (2015). Heat transfer and flow of a Casson fluid due to a stretching cylinder with the Soret and Dufour effects. *Journal of Engineering Physics and Thermophysics*, *88*, 928-936.
[27] Srinivasacharya, D., Mallikarjuna, B., & Bhuvanavijaya, R. (2015). Soret and Dufour effects on mixed convection along a vertical wavy surface in a porous medium with variable properties. *Ain Shams Engineering Journal*, *6*(2), 553-564.
[28] Ahmed, S. E., Arafa, A. A., & Hussein, S. A. (2024). Bioconvective flow of a variable properties hybrid nanofluid over a spinning disk with Arrhenius activation energy, Soret and Dufour impacts. *Numerical Heat Transfer, Part A: Applications*, *85*(6), 900-922.
[29] Balla, C. S., Ramesh, A., Kishan, N., & Rashad, A. M. (2021). Impact of Soret and Dufour on bioconvective flow of nanofluid in porous square cavity. *Heat Transfer*, *50*(5), 5123-5147.
[30] Razaq, A., Hayat, T., Khan, S. A., & Alsaedi, A. (2024). Radiative bioconvective flow with non-uniform heat source and Soret and Dufour impacts. *Alexandria Engineering Journal*, *98*, 159-169.
[31] Yin, J., Zhang, X., Rehman, M. I. U., & Hamid, A. (2022). Thermal radiation aspect of bioconvection flow of magnetized Sisko nanofluid along a stretching cylinder with swimming microorganisms. *Case Studies in Thermal Engineering*, *30*, 101771.
[32] Al-Mubaddel, F. S., Farooq, U., Al-Khaled, K., Hussain, S., Khan, S. U., Aijaz, M. O., ... & Waqas, H. (2021). Double stratified analysis for bioconvection radiative flow of Sisko nanofluid with generalized heat/mass fluxes. *Physica Scripta*, *96*(5), 055004.

[33] Puneeth, V., Manjunatha, S., Gireesha, B. J., & Shehzad, S. A. (2021). The three-dimensional bioconvective flow of Sisko nanofluid under Robin's conditions. *Heat Transfer*, *50*(8), 7632-7653.
[34] Raju, C. S. K., & Sandeep, N. (2016). Heat and mass transfer in MHD non-Newtonian bio-convection flow over a rotating cone/plate with cross diffusion. *Journal of molecular liquids*, *215*, 115-126.
[35] Hussain, A., Malik, M. Y., Salahuddin, T., Bilal, S., & Awais, M. (2017). Combined effects of viscous dissipation and Joule heating on MHD Sisko nanofluid over a stretching cylinder. *Journal of Molecular Liquids*, *231*, 341-352.
[36] Yin, J., Zhang, X., Rehman, M. I. U., & Hamid, A. (2022). Thermal radiation aspect of bioconvection flow of magnetized Sisko nanofluid along a stretching cylinder with swimming microorganisms. *Case Studies in Thermal Engineering*, *30*, 101771.